APPLICATIONS PAPER

Mapping Direct Seeded Rice in Raichur District of Karnataka, India

Murail Krishna Gumma, Deepika Uppala, Irshad A. Mohammed, Anthony M. Whitbread, and Ismail Rafi Mohammed

Abstract

Across South Asia, the cost of rice cultivation has increased due to labor shortage. Direct seeding of rice is widely promoted in order to reduce labor demand during crop establishment stage, and to benefit poor farmers. To facilitate planning and to track farming practice changes, this study presents techniques to spatially distinguish between direct seeded and transplanted rice fields using multiple-sensor remote sensing imagery. The District of Raichur, a major region in northeast Karnataka, Central India, where irrigated rice is grown and direct seeded rice has been widely promoted since 2000, was selected as a case study. The extent of cropland was mapped using Landsat-8, Moderate Resolution Imaging Spectroradiometer (MODIS) 16-day normalized difference vegetation index (NDVI) time-series data and the cultivation practice delineated using RISAT-1 data for the year 2014. Areas grown to rice were mapped based on the length of the growing period detected using spectral characteristics and intensive field observations. The high resolution imagery of Landsat-8 was useful to classify the rice growing areas. The accuracy of land-use/land-cover (LULC) classes varied from 84 percent to 98 percent. The results clearly demonstrated the usefulness of multiple-sensor imagery from MOD09Q1, Landsat-8, and RISAT-1 in mapping the rice area and practices accurately, routinely, and consistently. The low cost of imagery backed by ground survey, as demonstrated in this paper, can also be used across rice growing countries to identify different rice systems.

Introduction

Agriculture is an important sector in India, contributing about 17.9 percent of the gross domestic product (GDP) (2014 figures) (CIA, 2015). About 68 percent of the country's population lives in rural areas (FAOSTAT, 2013). India is one of the largest rice growing nations accounting for one quarter of the global rice area and produces around 125 million tons/year, with low yields of around 2.85 t/ha (Siddiq, 2000). Given that rice is a staple food crop in India and that the country has a population that is growing at 1.2 percent per annum, a substantial increase in rice production is the only way to guarantee food security and to keep food prices low. Labor and fertilizer are the two major input costs that are incurred while growing rice when there is assured water availability (Savary *et al.*, 2005). Migration from rural to urban areas in search of work has led to labor shortages and higher costs of agricultural operations (Hossain, 1998; Savary *et al.*, 2005). To overcome these constraints, promoting direct seeding in lieu of the traditional and labor-intensive transplanting (De Datta, 1986; Naylor, 1992) is being seen as a feasible alternative. However, there is a tradeoff with lower yields in rice that is direct seeded rather than transplanted; so efforts are on to bridge this gap (Khush, 1995).

Accurate and timely information on rice systems, cropped area, and yields are very important for sustainable food security. Several studies have used remote sensing data to monitor rice crop. Remote sensing technology provides a time saving approach to estimate cropped area, intensity and other LULC changes in a country (Badhwar, 1984; Gumma *et al.*, 2011a; Gumma *et al.*, 2015; Lobell *et al.*, 2003; Thenkabail *et al.*, 2009a; Thenkabail, 2010; Thiruvengadachari and Sakthivadivel, 1997). Many studies have reported the use of spatial-temporal data to map irrigated areas, land-use, land-cover, and crop type (Dheeravath *et al.*, 2010; Goetz *et al.*, 2004; Gumma *et al.*, 2014; Knight *et al.*, 2006; Thenkabail *et al.*, 2005; Varlyguin *et al.*, 2001; Velpuri *et al.*, 2009) using MODIS NDVI time-series data to map both agricultural areas (Biggs *et al.*, 2006; Gaur *et al.*, 2008; Gumma *et al.*, 2011c) and seasonal crop area (Sakamoto *et al.*, 2005). There are also studies that have used Synthetic Aperture Radar (SAR) data to monitor rice areas, particularly irrigated rice. (Le Toan *et al.*, 1997) used ERS-1 data as input to crop growth simulation models to estimate production for study sites in Indonesia and Japan. Similarly, (Shao *et al.*, 2001) mapped rice areas using temporal RADARSAT data (1996 and 1997) for production estimates in Zhaoqing in China. (Imhoff and Gesch, 1990) derived sub-canopy digital terrain models of flooded forest using SAR. (Kasischke and Bourgeau-Chavez, 1997) monitored the wetlands of South Florida using ERS-1 SAR imagery. (Leckie, 1990) distinguished forest type using SAR and optical data. (Robinson *et al.*, 2000) delineated drainage flow directions using SAR data. (Townsend, 2001) mapped seasonal flooding in forested wetlands using temporal RADARSAT SAR imagery. (Bouvet and Le Toan, 2011) demonstrated how lower resolution wide-swath images from advanced SAR (ASAR) data could be used to map rice over larger areas. (Uppala *et al.*, 2015) mapped rice areas using single data hybrid polarimetric data from RISAT-1 SAR data. The advantage of rice mapping with SAR is that it can overcome pervasive cloud cover across Asia during the rainy season months when rice is cultivated. However, its high cost inhibits its large-scale application.

A comprehensive plan to increase agricultural productivity and manage labor can be drawn up based on near real-time monitoring of rice systems along with weather and crop data acquired from an analysis of remote sensing imagery. Remote sensing platforms have proved to be ideal to take resource inventories and monitor agriculture. Interdisciplinary approaches and methods have made it easier to analyze imagery and extract information in ways unknown a few decades ago.

The goal of this study was to develop a method using multiple-sensor imagery (Landsat-8, RISAT-1 and MODIS time-series data) to map the spatial extent of two different rice cultivation practices (direct seeding and transplanting) in Raichur district, Karnataka State, India.

International Crops Research Institute for the Semi-Arid Tropics (ICRISAT), Patancheru, Telangana, India (m.gumma@cgiar.org).

Photogrammetric Engineering & Remote Sensing
Vol. 81, No. 11, November 2015, pp. 873–880.
0099-1112/15/873–880

doi: 10.14358/PERS.81.11.873

Study Area and Data Sets

Study Area

Raichur is one of largest and most productive rice growing district in Karnataka state in southern India (Figure 1). The district lies between 15°42'57" and 16°26'39" latitude and 76°14'47" and 77°35'39" longitude, with a land mass of 835,843 ha (cropped area 695,000 ha) (Figure 1) and bound in the north and south by the rivers Krishna and Tungabhadra. Agro-climatically, it falls under the Northeast Dry Zone of Karnataka (semi-arid eco-subregion) with a long term average rainfall of just above 600 mm distributed over *kharif* and *rabi* seasons. Much of the district is well irrigated by the Tungabhadra Dam on the Tungabhadra River, and the Narayanpura Dam on the Krishna River, covering an irrigated area of 185,000 ha, 72.2 percent of which is from canals. The arable rainfed area occupies 405,000 ha. The major crops grown in the district include paddy, sorghum, groundnut, sunflower, cotton, and pulses (chickpea and pigeonpea). The rice-rice cropping system is dominant in most irrigated areas. The soils of the district are mainly deep black clayey (47 percent) and red (34 percent).

Satellite Images

Four Landsat-8 tiles were downloaded from the Earth Explorer, global land cover facility website (*http://earthexplorer.usgs.gov/*). Images from the 2014 monsoon season and their spectral characteristics are shown in Table 1. All the Landsat-8 tiles were converted into reflectance (*http://landsat.usgs.gov/documents/Landsat8DataUsersHandbook.pdf*) to normalize the multi-date effect (Markham and Barker, 1986; Thenkabail *et al*., 2004) using the spatial modeler in ERDAS Imagine® (ERDAS, 2007). The 250-m, two-band MODIS data (centered at 648 nm and 858 nm; Table 1) collection 5 (MOD09Q1) were acquired for every eight days during the crop-growing seasons from January 2014 through December 2014. The data was acquired in 12-bit (0 to 4,096 levels) and stretched to 16-bit (0 to 65,536 levels). Further processing steps are described in (Gumma *et al*., 2015; Gumma *et al*., 2011b; Thenkabail *et al*., 2005).

RISAT-1, C-band (5.35 GHz) HH polarization, Medium Resolution SAR (MRS) temporal data sets were used to distinguish direct seeded rice from transplanted rice. Data was acquired every 25 days at a 37° angle of incidence spaced phenologically appropriate to identify rice fields and provide information on data sets (Table 1).

Ground Survey Data

A ground survey was conducted during the monsoon season for the crop year 2014 to 2015. Data was collected at 238 locations covering the major cropland areas in the study area. All location-specific data were collected from 250 × 250 meter plots and consisted of location coordinates (latitude, longitude), land-use categories, land-use (percent), cropping systems during the monsoon season (through farmer interviews), crop types, and watering method (irrigated/rainfed). Samples were within large contiguous areas of a specific land-use/land-cover. The locations were chosen based on pre-classification classes and local expertise. The local experts also provided information on cropping systems, cropping patterns and cropping intensity (single or double crop), irrigation application, and canopy cover (percent) for the previous years for these locations from their recorded data. Overall, 116 spatially well-distributed data points (Figure 1) were used for class identification and labeling; of these, 46 data points were used for ideal spectra generation and an additional 122 were used to assess accuracy.

Table 1. Characteristics of Multiple Satellite Sensor Data Used in the Study

Sensor	Dates	Spatial (m)	Bands	Band range (μm)
Landsat-8	07 & 14 Nov 2014	30	1	0.433–0.453
			2	0.450–0.515
			3	0.525–0.600
			4	0.630–0.680
			5	0.845–0.885
			6	1.560–1.660
			7	2.100–2.300
RISAT-1	28 Jun 2014; 23 Jul 2014; 17 Aug 2014; 11Sep 2014; 06 Oct 2014	18	1	HH polarization
MODIS (MOD09Q1)	2014 (16 days)	250	1	0.62–0.67
			2	0.84–0.88
			NDVI	- 1 to + 1

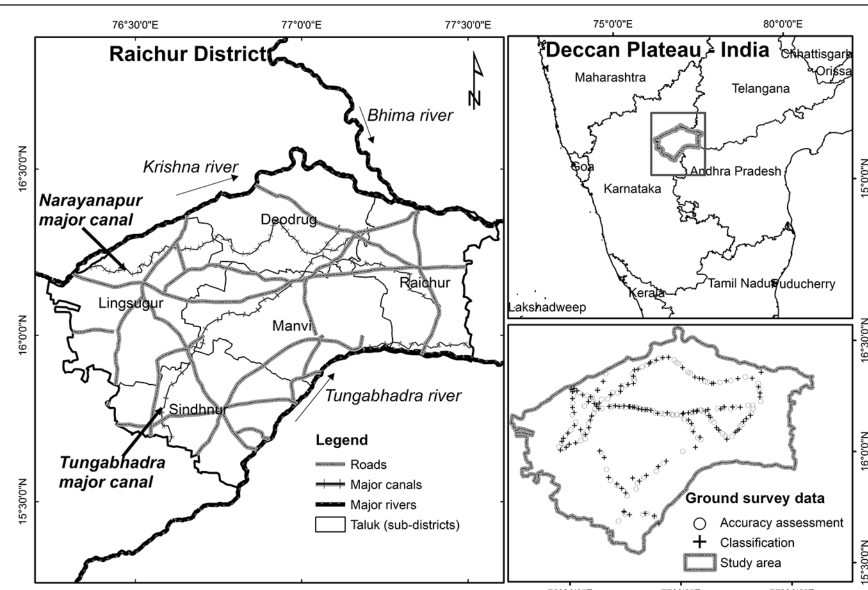

Figure 1. Raichur District, Karnataka, India.

Methods

Figure 2 presents an overview of the comprehensive methodology used to map direct seeded and transplanted rice cultivation practices using time series imagery from MOD09Q1 (spatial resolution 250 m) 16-day time-series NDVI, Landsat-8 (spatial resolution 30 m), and RISAT-1 (spatial resolution 18 m). Rice growing areas were delineated initially with MODIS time-series NDVI using spectral matching techniques (Gumma *et al.*, 2011b; Gumma *et al.*, 2014; Thenkabail *et al.*, 2007a). This was used as a mask to clip Landsat-8 time-series imagery. The subset of Landsat-8 was reclassified to separate rice from non-rice areas due to the difference in resolution between MODIS and Landsat-8. The Landsat-8 output provided a more accurate delineation of rice growing area. This subset was again used as a mask to clip out RISAT-1 temporal imagery.

Land-Use / Land-Cover Classification

The procedure began with image normalization of Landsat-8 data converted to top of atmosphere (TOA) reflectance using a reflectance model implemented in ERDAS Imagine (*http://landsat.usgs.gov/documents/Landsat8DataUsersHandbook.pdf*).

The (Operational Land Imager) OLI band data can be converted to TOA planetary reflectance using Reflectance rescaling coefficients provided in the product metadata file. The following equation was used to convert DN values to TOA planetary reflectance for OLI data:

$$\rho\lambda' = M_\rho Q_{cal} + A_\rho \quad (1)$$

where: $\rho\lambda'$ = TOA planetary reflectance (without correction of solar angle), M_ρ = Band specific multiplicative rescaling factor from the metadata, A_ρ = Band specific additive rescaling factor from the metadata, and Q_{cal} = the quantized and calibrated standard product pixel values (DN).

TOA reflectance with correction for the sun angle is then:

$$\rho\lambda = \frac{\rho\lambda'}{\sin(\theta_{SE})} \quad (2)$$

where: $\rho\lambda$ = TOA planetary reflectance, $\rho\lambda'$ = TOA planetary reflectance (without correction of solar angle), and θ_{SE} = the local sun elevation angle provided in the metadata.

The MODIS stacked composite was classified using unsupervised ISOCLASS cluster K-means classification algorithm followed by successive generalization (Biggs *et al.*, 2006; Gumma *et al.*, 2011c; Thenkabail *et al.*, 2005). The unsupervised classification algorithm (in ERDAS Imagine 2010) was applied on a 12-band NDVI (monthly Maximum Value Composite) MVC to obtain the initial 100 classes, followed by progressive generalization (Cihlar *et al.*, 1998). The unsupervised classification was set at a maximum of 100 iterations with a convergence threshold of 0.99 (Leica, 2010). Time-series NDVI spectra were then plotted for each of the 100 classes and compared with the ideal spectra to identify and label classes (Gumma *et al.*, 2014). However, the time-series NDVI profile helps gain an understanding of the growth profile of different crops in addition to providing information on planting date, discrimination between rice and other crops, early stage conditions (flooded pixel showing low values initially), and discrimination between irrigation sources (e.g., irrigated versus rainfed). Class identification and labeling were performed based on a suite of methods and ancillary data, such as decision tree algorithms, spectral matching techniques, Google Earth™ high-resolution imagery and ground survey data (Gumma *et al.*, 2014; Thenkabail *et al.*, 2009b; Thenkabail *et al.*, 2007b). The initial reduction in classes used a decision tree method (De Fries *et al.*, 1998) based on the temporal NDVI data. The decision tree is based on NDVI thresholds at different stages in the season that define vegetation growth cycle, and these algorithms help to identify similar classes. The dates and threshold values were derived from the ideal temporal profile (Gumma *et al.*, 2014). Using the ground survey data, Google Earth's high-resolution imagery along with spectral profiles of rice crops from MODIS imagery, Landsat-8 imagery was classified using the supervised maximum likelihood classification algorithm.

The MODIS-derived rice area was used as the basis of the maximum possible extent of rice area as one segment and other LULC areas as another segment. This was used as a mask to clip Landsat-8 time-series imagery. The subset of Landsat-8 was classified again to separate rice from non-rice areas. Both segments were classified independently (to avoid mixed classification) using the protocols mentioned earlier. This led to a more accurate delineation of rice growing area, but did not show fragmented direct seeded rice areas. This was mainly because direct seeded rice was sown in the early monsoon, when there were no images due to heavy clouds. Landsat-8 rice area was again used as a mask to clip out RISAT-1 temporal imagery. Separating the two practices of rice cultivation was possible using RISAT-1 temporal imagery. This is the best complimentary data to monitor croplands during the monsoon season, and where there are continuous clouds.

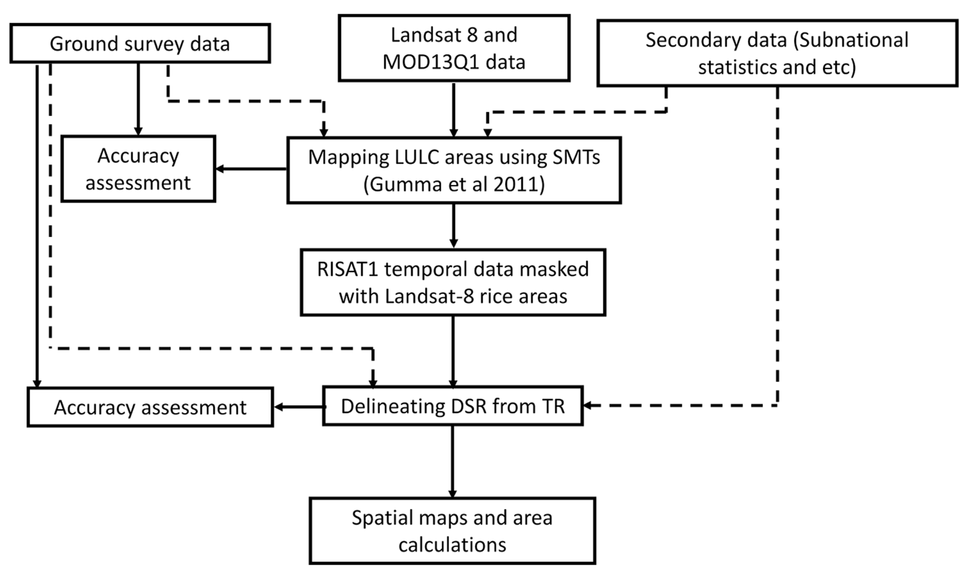

Figure 2. Overview of the methodology for mapping different rice growing practices.

Delineating Direct Seeded Rice (DSR) Cultivation Using SAR Data

The RISAT-1 data was processed using ENVI software. The level-2, HH polarization data was imported in ENVI raster format (.hdr). To reduce noise, Enhanced Lee Adaptive Speckle Filter with kernel size of 5 × 5 was applied (Lopes *et al.*, 1990). Radiometric calibration for HH polarization amplitude image was carried out by using the metadata provided along with the imagery. The scaled values of digital numbers were converted into backscattering coefficient using the equation given in (Chakraborty *et al.*, 2013; Laur *et al.*, 2002). The temporal images were co-registered by fitting a second order polynomial model to the manual GCPs with 50 well distributed points throughout the scene. The temporal HH polarization RISAT-1 data was stacked. The rice crop delineated from Landsat-8 was used to subset the RISAT-1 data stack for further processing.

In Raichur, direct seeded rice cropping is practiced along with transplanted rice which is most prevalent. Transplanted rice is of two types depending on sowing date. The early transplanted rice is sown in August and the late transplanted rice in September. SAR data is unique since it can distinguish between different rice sowing dates. The rice crop generates a unique temporal backscatter profile. It is clear from Figure 3 that during the establishment stage of transplanted rice, the backscatter is higher than direct seeded rice due to tilling and low moisture. During transplantation, backscatter is quite low due to standing water which reflects minimal energy in the backscatter direction. Further, the backscatter increases as the plant grows because of multiple reflections from the crop canopy (Choudhury *et al.*, 2012).

In the establishment phase of direct seeded rice, low backscatter was observed due to moisture conditions. This is the key to distinguishing 80 percent of the direct seeded rice from transplanted fields. Also, some of the transplanted rice fields cannot be distinguished from direct seeded fields due to high standard deviation in transplanted fields because of roughness. Additionally, early transplanted rice could be

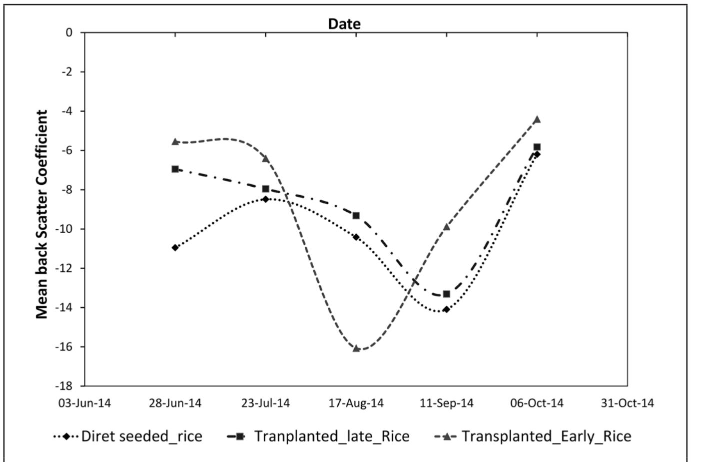

Figure 3. Temporal changes in backscatter coefficient in different rice growing practices.

distinguished at the transplantation stage due to very low backscatter. However, it is difficult to discriminate between direct seeded rice and late transplantation due to their similar growth stages. The deviation of backscatter was found to be low. The decision tree hybrid classification algorithm was used here in order to separate the above mixed classes. June is the crucial month to separate transplanted rice form direct seeded rice (80 percent). The early transplanted rice was easily separated from directed seeded rice by applying decision rules on the August imagery. This was possible because the difference in backscatter was more than 2 dB. The late transplantation was not separable from direct seeded rice because of the low difference in backscatter. In order to resolve these types of fields, unsupervised k-means algorithm with a convergence threshold of 0.99 was applied on the remaining area

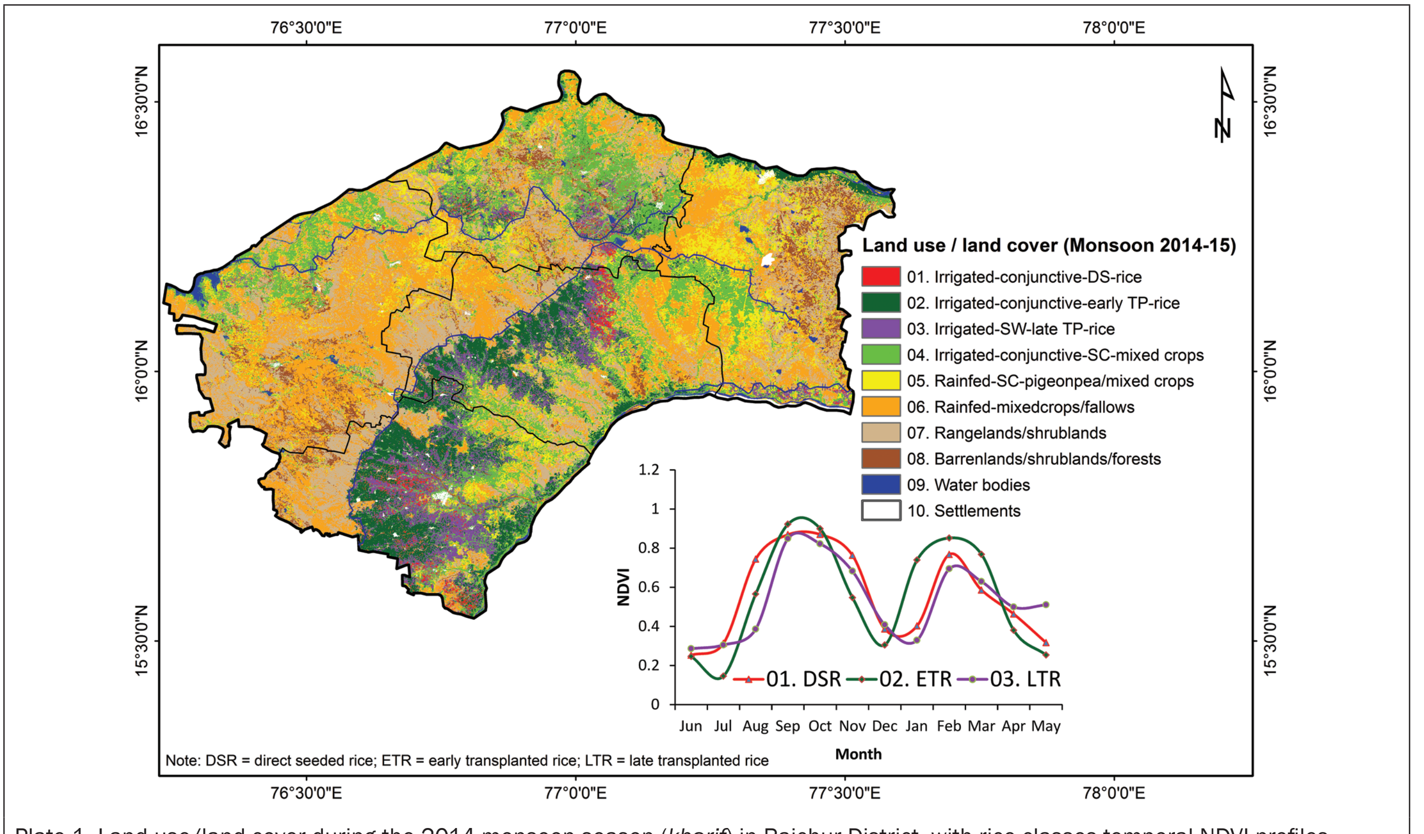

Plate 1. Land-use/land-cover during the 2014 monsoon season (*kharif*) in Raichur District, with rice classes temporal NDVI profiles.

which included late transplanted rice and direct seeded rice. By using this algorithm, 85 percent of late transplanted rice fields were separated from direct seeded rice fields.

Results

Spatial Distribution of Land Use / Land Cover

Ten land-use/land-cover classes were identified using spectral matching techniques using MODIS temporal imagery and Landsat-8 (Plate 1). With average rainfall in the order of 600 mm/annum and large areas under rainfed cropping, canal irrigation from Tungabhadra Dam provides insufficient irrigation to grow rice. The total irrigated area accounts for 287,993 ha (Table 2). The important rice growing taluks (administrative units) are Manvi and Sindhanur where a large area is irrigated under rice. The adoption of direct rice seeding is due to shortage of labor, and it is a new phenomenon and expanding along with transplanted rice cultivation which is essentially large in extent. The use of temporal RISAT-1 imagery helped in identifying how rice was planted (direct seeded rice or transplanted) and also ascertaining time of planting (early or late transplanting). This information can be used to schedule irrigation and estimate harvest dates for each type of practice. It is clear that the head end of the canal has a larger extent of transplanted rice than the tail end in Manvi and Sindhanur with irrigated mixed crops. Rainfed croplands occupy the largest area of 351,895 ha in Raichur District. Pigeonpea mixed with a cereal crop like sorghum is one of the important and large cropping systems in the taluks of Lingsugur and Raichur. Rangelands and shrublands are comparably large which can be potentially used for rainfed agriculture.

Table 2. Estimated Area Under Different Land Use/Land Cover (LULC) Classes in Raichur District

LULC area	Area (ha)	%
01. Irrigated-conjunctive-DS-rice	12,942	1.5
02. Irrigated-conjunctive-early TP-rice	67,418	8.0
03. Irrigated-SW-late TP-rice	49,983	5.9
04. Irrigated-conjunctive-SC-mixed crops	157,650	18.7
05. Rainfed-SC-pigeonpea/mixed crops	122,778	14.6
06. Rainfed-mixed crops/fallows	229,117	27.2
07. Rangelands/shrublands	152,442	18.1
08. Barren lands/shrublands/forests	37,060	4.4
09. Water bodies	9,241	1.1
10. Settlements	3,695	0.4
Total	842,326	

Spatial Extent of Direct Seeded Rice and Transplanted Rice

Rice is a major crop in Raichur District, covering 130,343 ha in 2013, out of which transplanted rice covered 117,401 ha and direct seeded rice 12,942 ha. The major rice area is located in Manvi and Sindhanur taluks which are irrigated, depending on ground water availability and rainfall. Of the total rice area, 52 percent is early transplanted rice, 38 percent is late transplanted rice, and only 10 percent is direct seeded rice (Table 2 and Plate 1). Variations within the direct seeded field are difficult to identify due to the temporal deficit of the image acquisition.

Accuracy Assessment

The classification accuracies obtained from the 122 independent ground data observation data points for the year 2014 were gathered from the study area (monsoon season). Accuracy assessment was done using error matrix, a multi-dimensional table in which the cells contain changes from one land-use class to another. The statistical approach of accuracy assessment consists of different multi-variate statistical analyses (Congalton and Green, 1999; Jensen, 1996). The error matrix accuracy varied from 75 percent to 92 percent across six cropland areas. However, it must be noted that rice classes did not mix with other classes. Overall, accuracy was 82 percent and kappa was 0.78. So the uncertainty of about 18 percent is due to the inter-mix among the other land-use/land-cover classes (Table 3).

Comparison with National Statistics and Other Studies

Statistics on taluk-wise rice area in Raichur District was obtained from the Bureau of Economics and Statistics, Government of Karnataka State, India. This data was used for comparing RISAT-1, Landsat-8, and MODIS-derived statistics. A high correlation was found (Figure 4) between the two sources of information on rice cultivation in the district.

Table 3. Accuracy Assessment Using Ground Survey Data (Two Dimensional Error Matrix)

	Reference data											
Classified data	01. Irrigated-conjuctive-DS-rice	02. Irrigated-conjunctive-early TP-rice	03. Irrigated-SW-late TP-rice	04. Irrigated-conjunctive-SC-mix	05. Rainfed-SC-pigeonpea / mixed crops	06. Rainfed-mixed crops/fallows	07. Other LULC	**Reference row total**	**Classified totals**	**Producers accuracy**	**Users accuracy**	**Kappa accuracy**
01. Irrigated-conjuctive-DS-rice	3	0	1	0	0	0	0	3	4	100%	75%	74%
02. Irrigated-conjuctive-early TP-rice	0	12	1	0	0	0	0	13	13	92%	92%	91%
03. Irrigated-SW-late TP-rice	0	0	7	1	0	0	0	9	8	78%	88%	87%
04. Irrigated-conjuctive-SC-mix	0	0	0	22	2	1	0	24	25	92%	88%	85%
05. Rainfed-SC-pigeonpea/mixed crops	0	0	0	1	19	2	1	27	23	70%	83%	78%
06. Rainfed-mixed crops/fallows	0	1	0	0	4	30	1	37	36	81%	83%	76%
07. Other LULC	0	0	0	0	2	4	7	9	13	78%	54%	50%
Total	3	13	9	24	27	37	9	122	122	84%	80%	77%

Discussion

Microwave remote sensing satellites carrying Synthetic Aperture RADAR (SAR) enable imaging of the features of the Earth's surface both during the day and the night under all weather conditions. These specific characteristics of the satellite are useful in identifying crop information under cloudy skies using standard methods. However, the objective stated in this study demands a hybrid approach where optical and SAR imagery are used to distinguish between the two rice growing practices that exhibit similar backscatter mechanisms, except at the establishment stage. Studies have been conducted to come up with a robust classification method using X-band SAR data to map rice crops, including for direct seeding in different ecosystems and also to examine the relationship between crop characteristics and backscatter coefficient (Nelson *et al.*, 2014). However, the inherent property of C-band SAR data, where the wavelength responds to roughness of soil by including any background (soil backscatter), makes a difference by identifying a practice like direct seeded rice. The basic premise that direct seeded rice requires less labor and less water, making it economically less demanding option and also a strategy to cope with monsoon failure, has some lacunae. This is because the direct seeded rice fields are more infested by weeds than transplanted rice fields (Rao *et al.*, 2007) as the puddled fields do not allow weed growth. This leads to yield losses depending on weed infestation.

RISAT-1 SAR imagery was a viable and useful option as it overcomes cloud cover as well as provides a convenient temporal coverage to distinguish between these two practices right at establishment stage. Mixed classes were resolved based on extensive ground information collected during field trips and tools like Google Earth Explorer™. A multi-sensor approach was a useful strategy to fulfill the objective of this study, especially to arrive at accurate estimates of the practice of growing direct seeded rice in Raichur District. The MODIS, 16-day NDVI data was primarily used to delineate the rice cropped areas taking advantage of its temporal availability. The spectral profiles from MODIS temporal data provide important information on different aspects of the crop, such as its source of water, phenological stage, and stress. The role of Landsat-8 imagery was to generate a high accuracy rice cropped area map to match the resolution of RISAT-1 imagery and in turn transfer information from MODIS to RISAT-1.

Karnataka State's sub-district divisions are large and few. For instance, Raichur has only five taluks. Statistics generated from this study on taluk-wise rice cropped area were compared with those from the government department. A high correlation was observed between these two sources of information (Figure 4). Statistics on direct seeded rice was not available from the government departments since it is a new practice in this district. However, this study was successful in identifying direct seeded rice because of the difference in crop establishment dates compared to the other practice of transplanting rice.

Conclusions

Mapping the cropped area of direct seeded rice using a multi-sensor approach, specifically the use of RISAT-1 imagery, is important as it can penetrate cloud cover during the rainy season. Optical remote sensing methods may not be successful in discriminating land-use classes based on management practices. Hybrid approaches have always proved useful in atypical cases such as this study. Even though there are three types of direct seeded rice cultivation, an attempt was made to map only the dry seeded sowing practice prevalent in Raichur District. Sindhanur and Manvi are the two taluks in the district where the practice is followed. Using the temporal SAR data along with optical data such as MODIS, a similar approach can be used to map direct seeded rice cultivation during post-rainy (*rabi)* season as well. The spatial distribution and quantification of the extent of direct seeded rice will not only help breeders to understand the locale-specific constraints to yields such as weeds, but also provide remedies to bridge the yield gaps. In turn, this will help in overcoming the labor shortage and also help in conserving water for other uses. In this context, it is proposed to study and examine how we can differentiate between rice establishment practices not only at the time of establishment using SAR imagery, but also when there is a large outbreak of weeds in direct seeded rice cultivation.

Acknowledgments

This research was supported by the CGIAR Research Program Water, Land and Ecosystems. The authors would like to thank Smitha Sitaraman and Amit Chakravarty, science editors/publisher at ICRISAT for his assistance with editing. The authors also thank Dr. AN Rao (IRRI) and Dr. Gajanan Sawargaonkar for their valuable feedback of the rice classification system and sub-district wise statistics.

References

Badhwar, G.D., 1984. Automatic corn-soybean classification using landsat MSS data - I. Near-harvest crop proportion estimation, *Remote Sensing of Environment*, 14(1-3):15–29.

Biggs, T.W., P.S. Thenkabail, M.K. Gumma, C.A. Scott, G.R. Parthasaradhi, and H.N. Turral, 2006. Irrigated area mapping in heterogeneous landscapes with MODIS time series, ground truth and census data, Krishna Basin, India, *International Journal of Remote Sensing*, 27(19):4245–4266.

Bouvet, A., and T. Le Toan, 2011. Use of ENVISAT/ASAR wide-swath data for timely rice fields mapping in the Mekong River Delta, *Remote Sensing of Environment*, 115(4):1090–1101.

Chakraborty, M., S. Panigrahy, A. Rajawat, R. Kumar, T. Murthy, D. Haldar, A. Chakraborty, T.

Kumar, S. Rode, and H. Kumar, 2013. Initial results using RISAT-1 C-band SAR data, *Current Science* (Bangalore), 104(4):490–501.

Choudhury, I., M. Chakraborty, S.C. Santra, and J.S. Parihar, 2012. Methodology to classify rice cultural types based on water regimes using multi-temporal RADARSAT-1 data, *International Journal of Remote Sensing*, 33(13):4135–4160.

CIA, 2015. The World Factbook, URL: *https://www.cia.gov/library/publications/the-world-factbook/fields/2012.html* (last date accessed: 24 September 2015).

Cihlar, J., Q. Xiao, J. Beaubien, K. Fung, and R. Latifovic, 1998. Classification by progressive generalization: A new automated methodology for remote sensing multichannel data, *International Journal of Remote Sensing*, 19(14):2685–2704.

Congalton, R.G., and K. Green, 1999. *Assessing the Accuracy of Remotely Sensed Data: Principles and Practices*, New York: Lewis.

De Datta, S., 1986. Technology development and the spread of direct-seeded flooded rice in Southeast Asia, *Experimental Agriculture*, 22(04):417–426.

De Fries, R.S., M. Hansen, J.R.G. Townshend, amd R. Sohlberg, 1998. Global land cover classifications at 8 km spatial resolution: The use of training data derived from Landsat imagery in decision tree classifiers, *International Journal of Remote Sensing*, 19(16):3141–3168.

Dheeravath, V., P.S. Thenkabail, G. Chandrakantha, P. Noojipady, G.P.O. Reddy, C.M. Biradar, M.K. Gumma, and M. Velpuri, 2010. Irrigated areas of India derived using MODIS 500 m time series for the years 2001-2003, *ISPRS Journal of Photogrammetry and Remote Sensing*, 65(1):42–59.

ERDAS, 2007. *ERDAS Field Guide*, Volume 1, October 2007.

FAOSTAT, 2013. URL: http://faostat.fao.org/site/666/default.aspx (last date accessed: 24 September 2015).

Gaur, A., T.W. Biggs, M.K. Gumma, and H. Turral, 2008. Water scarcity effects on equitable water distribution and land use in Major Irrigation Project - A Case study in India, *Journal of Irrigation and Drainage Engineering*, 134 (1):26–35.

Goetz, S.J., D. Varlyguin, A.J. Smith, R.K. Wright, S.D. Prince, M.E. Mazzacato, J. Tringe, C. Jantz, and B. Melchoir, 2004. Application of multitemporal Landsat data to map and monitor land cover and land use change in the Chesapeake Bay watershed, *Analysis of Multi-temporal Remote Sensing Images* (P. Smits and L. Bruzzone, editors), World Scientific Publishers, Singapore, pp. 223–232.

Gumma, M.K., S. Mohanty, A. Nelson, R. Arnel, I.A. Mohammed, and S.R. Das, 2015. Remote sensing based change analysis of rice environments in Odisha, India, *Journal of Environmental Management*, 148(0):31–41.

Gumma, M.K., P.S. Thenkabail, A. Maunahan, S. Islam, and A. Nelson, 2014. Mapping seasonal rice cropland extent and area in the high cropping intensity environment of Bangladesh using MODIS 500m data for the year 2010, *ISPRS Journal of Photogrammetry and Remote Sensing*, 91(5):98–113.

Gumma, M.K., D. Gauchan, A. Nelson, S. Pandey, and A. Rala, 2011a. Temporal changes in rice-growing area and their impact on livelihood over a decade: A case study of Nepal, *Agriculture, Ecosystems & Environment*, 142(3-4):382–392.

Gumma, M.K., A. Nelson, P.S. Thenkabail, and A.N. Singh, 2011b. Mapping rice areas of South Asia using MODIS multitemporal data, *Journal of Applied Remote Sensing*, 5, 053547.

Gumma, M.K., P.S. Thenkabail, I.V. Muralikrishna, M.N. Velpuri, P.T. Gangadhararao, V. Dheeravath, C.M. Biradar, S. Acharya Nalan, and A. Gaur, 2011c. Changes in agricultural cropland areas between a water-surplus year and a water-deficit year impacting food security, determined using MODIS 250 m time-series data and spectral matching techniques, in the Krishna River basin (India), *International Journal of Remote Sensing*, 32(12):3495–3520.

Hossain, M., 1998. *Sustaining Food Security in Asia: Economic, Social, and Political Aspects - Sustainability of Rice in the Global Food System*, Pacific Basin Study Center, Davis, California, and International Rice Research Institute, Manila, The Philippines, pp. 19–44.

Imhoff, M.L., and D.B. Gesch, 1990. The derivation of a sub-canopy digital terrain model of a flooded forest using synthetic aperture radar, *Photogrammetric Engineering & Remote Sensing*, 56(8):1155–1162.

Jensen, J.R., 1996. *Introductory Digital Image Processing: A Remote Sensing Perspective*, Prentice Hall, Upper Saddle River, New Jersey.

Kasischke, E.S., and L.L. Bourgeau-Chavez, 1997. Monitoring south Florida wetlands using ERS-1 SAR imagery, Photogrammetric Engineering & Remote Sensing 63(3):281–291.

Khush, G.S., 1995. Breaking the yield frontier of rice, *GeoJournal*, 35(3):329–332.

Knight, J.F., R.L. Lunetta, J. Ediriwickrema, and S. Khorram, 2006. Regional scale land-cover characterization using MODIS-NDVI 250 m multi-temporal imagery: A phenology based approach, *GIScience and Remote Sensing*, 43(1):1–23.

Laur, H., P. Bally, P., Meadows, J. Sanchez, B. Schaettler, E. Lopinto, and D. Esteban, 2002.

Derivation of the backscattering coefficient θ0 in ESA ERS SAR PRI products, ESA, Noordjiwk, The Netherlands, ESA Document ES-TN-RE-PM-HL09(2).

Le Toan, T., F. Ribbes, L.-F. Wang, N. Floury, K.-H. Ding, J.A. Kong, M. Fujita, and T. Kurosu, 1997. Rice crop mapping and monitoring using ERS-1 data based on experiment and modeling results, *IEEE Transactions on Geoscience and Remote Sensing*, 35(1):41–56.

Leckie, D., 1990. Synergism of synthetic aperture radar and visible/infrared data for forest type discrimination, *Photogrammetric Engineering & Remote Sensing*, 56(9):1237–1246.

Leica, 2010. *ERDAS Field Guide*, Volume 4, October 2010.

Lobell, D.B., G.P. Asner, J.I. Ortiz-Monasterio, and T.L. Benning, 2003. Remote sensing of regional crop production in the Yaqui Valley, Mexico: Estimates and uncertainties, Agriculture, Ecosystems & Environment 94(2):205–220.

Lopes, A., R. Touzi, and E. Nezry, 1990. Adaptive speckle filters and scene heterogeneity, *IEEE Transactions on Geoscience and Remote Sensing*, 28(6):992–1000.

Markham, B.L., and J.L. Barker, 1986. *Landsat MSS and TM Post - Calibration Dynamic Ranges, Exoatmospheric Reflectances and At-Satellite Temperatures*, Earth Observation Satellite Company, Lanham, Maryland, Landsat Technical Notes, 1, August.

Naylor, R., 1992. Labour-saving technologies in the Javanese rice economy: Recent developments and a look into the 1990s, *Bulletin of Indonesian Economic Studies*, 28(3):71–91.

Nelson, A., T. Setiyono, A.B. Rala, E.D. Quicho, J.V. Raviz, P.J. Abonete, A.A. Maunahan, C.A. Garcia, H.Z.M. Bhatti, and L.S. Villano, 2014. Towards an operational SAR-based rice monitoring system in Asia: Examples from 13 demonstration sites across Asia in the RIICE Project, *Remote Sensing*, 6(11):10773–10812.

Rao, A.N., D.E. Johnson, B. Sivaprasad, J.K. Ladha, and A.M. Mortimer, 2007. Weed management in directθseeded rice, *Advances in Agronomy* (L.S.Donald, editor), Academic Press, pp. 153–255.

Robinson, C., F. El-Baz, M. Ozdogan, M. Ledwith, D. Blanco, S. Oakley, and J. Inzana, 2000.

Use of radar data to delineate palaeodrainage flow directions in the Selima Sand Sheet, Eastern Sahara, *Photogrammetric Engineering & Remote Sensing*, 66(6):745–753.

Sakamoto, T., M. Yokozawa, H. Toritani, M. Shibayama, N. Ishitsuka, and H. Ohno, 2005. A crop phenology detection method using time-series MODIS data, *Remote Sensing of Environment*, 96(3-4):366–374.

Savary, S., N.P. Castilla, F. Elazegui, and P.S. Teng, 2005. Multiple effects of two drivers of agricultural change, labour shortage and water scarcity, on rice pest profiles in tropical Asia, *Field Crops Research*, 91(2):263–271.

Shao, Y., X. Fan, H. Liu, J. Xiao, S. Ross, B. Brisco, R. Brown, and G. Staples, 2001. Rice monitoring and production estimation using multitemporal RADARSAT, *Remote Sensing of Environment*, 76(3):310–325.

Siddiq, E., 2000. *Bridging the Rice Yield Gap in India*, URL: *http://www.fao.org/docrep/003/X6905E/x6905e09.htm* (last date accessed: 24 September 2015).

Thenkabail, P.S., 2010. Global croplands and their importance for water and food security in the twenty-first century: Towards an ever green revolution that combines a second green revolution with a blue revolution, *Remote Sensing*, 2(9):2305–2312.

Thenkabail, P., C. Biradar, P. Noojipady, V. Dheeravath, Y. Li, M. Velpuri, M. Gumma, G.

Reddy, H. Turral, X. Cai, J. Vithanage, M. Schull, and R. Dutta, 2009a. Global irrigated area map (GIAM) for the end of the last millennium derived from remote sensing, *International Journal of Remote Sensing,* 30(14):3679–3733.

Thenkabail, P.S., C.M. Biradar, P. Noojipady, V. Dheeravath, Y. Li, M. Velpuri, M., Gumma, O.R.P. Gangalakunta, H. Turral, X. Cai, J. Vithanage, M.A. Schull, and R. Dutta, 2009b. Global irrigated area map (GIAM), derived from remote sensing, for the end of the last millennium, *International Journal of Remote Sensing*, 30(14):3679–3733.

Thenkabail, P., P. GangadharaRao, T. Biggs, M. Gumma, and H. Turral, 2007a. Spectral matching techniques to determine historical land-use/land-cover (LULC) and irrigated areas using time-series 0.1-degree AVHRR Pathfinder datasets, *Photogrammetric Engineering & Remote Sensing*, 73(10):1029–1040.

Thenkabail, P.S., P. GangadharaRao, Y. Biggs, M.K. Gumma, and H. Turral, 2007b. Spectral Matching techniques to determine historical land use/land cover (LULC) and irrigated areas using time-series AVHRR Pathfinder datasets in the Krishna River Basin, India, *Photogrammetric Engineering and Remote Sensing*, 73(10):1029–1040.

Thenkabail, P.S., M. Schull, and H. Turral, 2005. Ganges and Indus river basin land use/land cover (LULC) and irrigated area mapping using continuous streams of MODIS data, *Remote Sensing of Environment*, 95(3):317–341.

Thenkabail, P.S., E.A. Enclona, M.S. Ashton, C. Legg, and M.J. De Dieu, 2004. Hyperion, IKONOS, ALI, and ETM+ sensors in the study of African rainforests, *Remote Sensing of Environment*, 90(1):23–43.

Thiruvengadachari, S., and R. Sakthivadivel, 1997. Satellite remote sensing for assessment of irrigation system performance: A case study in India, *Research Report 9*, Colombo, Sri Lanka: International Irrigation Management Institute.

Townsend, P.A., 2001. Mapping seasonal flooding in forested wetlands using multi-temporal Radarsat SAR, Photogrammetric Engineering & Remote Sensing, 67(7):857–864.

Uppala, D., R.V. Kothapalli, S. Poloju, S.S.V.R. Mullapudi, and V.K. Dadhwal, 2015. Rice crop discrimination using single date RISAT1 hybrid (RH, RV) polarimetric data, *Photogrammetric Engineering & Remote Sensing*, 81(7):557–563.

Varlyguin, D., R. Wright, S.J. Goetz, and S.D. Prince, 2001. Advances in land cover classification: A case study from the mid-Atlantic region, American Society for Photogrammetry and Remote Sensing, *Proceedings of the Annual Conference*, St. Louis, Missouri.

Velpuri, N.M., P.S. Thenkabail, M.K. Gumma, C.B. Biradar, P. Noojipady, V. Dheeravath, and L. Yuanjie, 2009. Influence of resolution in irrigated area mapping and area estimations, *Photogrammetric Engineering & Remote Sensing*, 75(12):1383–1395.

FORTHCOMING ARTICLES

Wei Li, *Kaichang Di*, *Zongyu Yue*, *Yiliang Liu*, and *Shujuan Sun*, Automated Detection of Martian Gullies from HiRISE Imagery.

Benjamin W. Heumann, The Multiple Comparison Problem in Empirical Remote Sensing.

Xinming Tang, *Ping Zhou*, *Guo Zhang*, and *Xia Wang*, Geometric Accuracy Analysis Model of the Ziyuan-3 Satellite without GCPs.

Tingting Liu, *Zemin Wang*, *Xin Huang*, *Liqin Cao*, *Muye Niu*, and *Zhongxiang Tian*, An Effective Antarctic Ice Surface Temperature Retrieval Method for MODIS.

Naizhuo Zhao, *Eric L. Samson*, and *Nathan A. Currit*, Nighttime Lights-derived Fossil Fuel Carbon Dioxide Emission Maps and Their Limitations.

Murali Krishna Gumma, *Deepika Uppala*, *Irshad A. Mohammed*, *Anthony M. Whitbread*, and *Ismail Rafi Mohammed*, Mapping Direct Seeded Rice in Raichur District of Karnataka, India.

Stephane Bertin, *Heide Friedrich*, and *Patrice Delmas*, A Merging Solution for Close-Range DEMS to Optimize Surface Coverage and Measurement Resolution.

Alireza Sharifi and *Jalal Amini*, Estimation of Forest Biomass Using Multivariate Relevance Vector Regression.

Quan Zhang, *Qinke Yang*, and *Chunmei Wang*, SRTM Error Distribution and its Associations with Landscapes across China.

Fateme Ameri, *Mohammad Javad Valadan Zoej*, and *Mehdi Mokhtarzade*, Multi-Criteria, Graph-Based Road Centerline Vectorization Using Ordered Weighted Averaging Operators.

Mi Wang, *Shenggu Yuan*, *Jun Pan*, *Liuyang Fang*, *Qinghua Zhou*, and *Guopeng Yang*, Seamline Determination for High Resolution Orthoimage Mosaicking Using Watershed Segmentation.

Matthew Maimaitiyiming, *Allison J. Miller*, and *Abduwasit Ghulam*, Discriminating Spectral Signatures Among and Within Two Closely Related Grapevine Species.

Min Wang and *Jie Wang*, A Region-Line Primitive Association Framework for Object-Based Remote Sensing Image Analysis.

Luigi Barazzetti, Sliver Removal in Object-Based Change Detection from VHR Satellite Images.

Ting On Chan, *Derek D. Lichti*, *David Belton*, and *Hoang Long Nguyen*, Automatic Point Cloud Registration Using a single Octagonal Lamp Pole.

John W. Coulston, *Christine E. Blinn*, *Valerie A. Thomas*, and *Randolph H. Wynne*, Approximation Prediction Uncertainty for Random Forest Regression Models.

Bonnie Ruefenacht, Comparison of Three Landsat-TM Compositing Methods: A Case Study Using Modeled Tree Canopy Cover.

Ahmed Izadipour, *Behzad Akbari*, and *Barat Mojaradi*, A Feature Selection Approach for Segmentation of Very High-Resolution Satellite Images.